

## FEASIBILITY STUDY OF RESIDUAL STRESS MEASUREMENT USING PHASED ARRAY ULTRASONIC METHOD

Yashar Javadi<sup>a,b,\*</sup>, Alistair Hutchison<sup>a</sup>, Rastislav Zimmermann<sup>a</sup>, Jonathan Singh<sup>a</sup>, Ehsan Mohseni<sup>a</sup>, Salaheddin Rahimi<sup>c</sup>, Jorn Mehnen<sup>b</sup>, Charles MacLeod<sup>a</sup>, Gareth Pierce<sup>a</sup>, Katherine Tant<sup>a</sup>, and Anthony Gachagan<sup>a</sup>

<sup>a</sup>Centre for Ultrasonic Engineering (CUE), Department of Electronic & Electrical Engineering (EEE),  
University of Strathclyde, Glasgow G1 1XQ, UK

<sup>b</sup>Department of Design, Manufacturing & Engineering Management (DMEM), University of Strathclyde,  
Glasgow G1 1XQ, UK

<sup>c</sup>Advanced Forming Research Centre (AFRC), University of Strathclyde, Renfrew PA4 9LJ, UK

---

### ABSTRACT

Residual stress measurement using the ultrasonic method is based on the acoustoelasticity law, which states that the Time-of-Flight (ToF) of an ultrasonic wave is affected by the stress field. Traditionally, single-element ultrasonic transducers are used for residual stress measurement. In this paper, a Phased Array Ultrasonic Testing (PAUT) system is used and the single element transducers are replaced by 5 MHz and 10 MHz arrays with 8 and 16 elements, respectively. The 10 MHz transmitter array can generate 16 ultrasonic waves and each of them can be received by any of the 16 elements of the 10 MHz receiver array. Therefore, a matrix of  $16 \times 16$  acoustic paths can potentially be generated. Each of these 256 LCR paths is different from the others (i.e., different distance or different position of the travel path in the material) whereby 256 ToFs can be generated. This is anticipated to increase the measurement accuracy in comparison with the traditional setup in which only two acoustic paths can be generated by using three single element transducers. In this paper, a feasibility study is conducted to investigate the requirements of a residual stress measurement system using the PAUT method. An advanced processing algorithm is also developed to analyse Full Matrix Capture (FMC). Based on the preliminary results, some variations between different acoustic paths are measured which prove that the effect of the residual stress on the ultrasonic wave is detectable using the PAUT system. Furthermore, the potential of this system for robotic residual stress measurement is discussed.

**Keywords:** Residual Stress; Phased Array Ultrasonic Testing (PAUT); Robotics; Waves; Welding; Wire Arc Additive Manufacturing (WAAM).

---

### 1. Introduction

Residual Stresses (RS) can be produced in a variety of manufacturing processes, from welding [1] and additive manufacturing [2] to forming [3] and machining [4]. They, along with the presence of undetected defects, can dangerously lower the applied stress threshold at which unexpected structural failure will occur [5]. The RS could also trigger the formation of other defects, for example, Javadi et al [1] showed that an excessive amount of 78 MPa in the RS can result in a considerable increase in the size of a hydrogen-induced crack from 2 mm to 13 mm. This can be even more concerning in Wire + Arc Additive Manufacturing (WAAM) process in which a near-yield tensile RS for aluminium and Inconel (around 1000 MPa) was reported by

---

\* Corresponding author. yashar.javadi@strath.ac.uk

Hönnige et al [6]. Therefore, the mitigation of RS is a critical procedure, especially in safety-critical components [7], however, they first need to be measured.

The measurement of welding and WAAM residual stresses can be achieved through non-destructive methods (e.g., ultrasonic techniques [8], which is the method used in this paper), semi-destructive methods (e.g., hole-drilling [7], which is the only standardised method by ASTM E837 [9]) or destructive methods (e.g., the contour method [10]). In this paper, the ultrasonic method is used, and improved through the Phased Array Ultrasonic Testing (PAUT) approach, to investigate the requirements for a RS measurement system developed for welding and WAAM components.

## 2. RS measurement using the ultrasonic method

The ultrasonic method for residual stress measurement works based on the acoustoelasticity law, which states that the material stress can affect the Time-of-Flight (ToF) of the ultrasonic wave. Egle and Bray [11] showed that the Longitudinal Critically Refracted (LCR) waves have a higher sensitivity to the stress in comparison with other types of ultrasonic wave. Based on the LCR method, Fig. 1a, the material stress ( $\sigma$ ) can be calculated if the acoustoelastic coefficient ( $L$ ), the ultrasonic wave ToF in both the stress-free material ( $T_1$ ) and material with the applied or residual stress ( $T_2$ ), are measured. It is also possible to penetrate various thicknesses of the material using different ultrasonic frequencies (Fig. 1b) to measure the through-thickness residual stress [8, 12]. The ultrasonic transducers (transmitter and receiver) are placed in a specially-designed wedge that can be freely moved over the component surface to extend the measurement coverage throughout the component. The acoustoelastic coefficient ( $L$ ) is a material property that is required to be measured during a controlled loading/unloading procedure, like the standard tensile test [8], as shown in Fig. 1c.

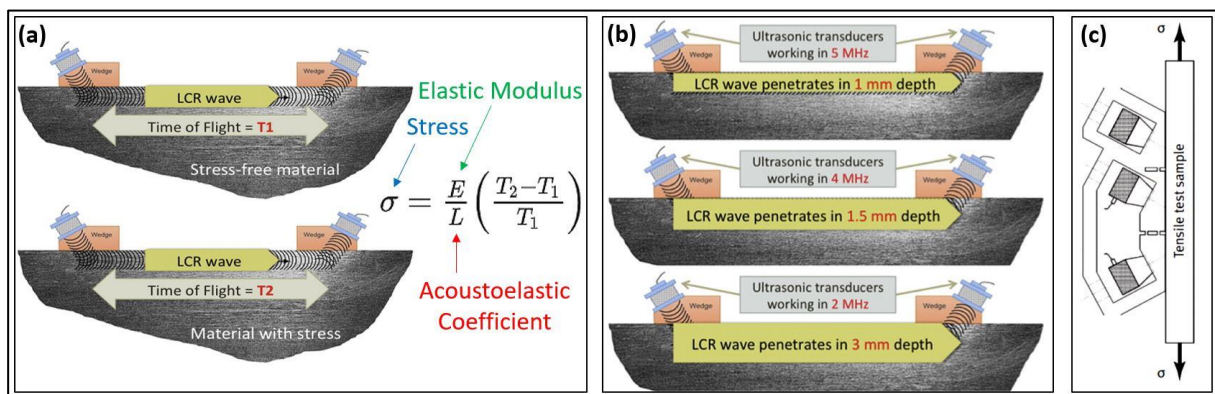


Fig. 1. (a) Principles of the ultrasonic stress measurement [12], (b) the possibility of through-thickness stress measurement [12] and (c) tensile test for measurement of the acoustoelastic coefficient [8]

The traditional system of LCR ultrasonic stress measurement is very sensitive to the material texture and temperature which affect the accuracy of the residual stress measurement [12]. In this paper, the PAUT system is used for the ultrasonic residual stress measurement rather than the single element as shown in Fig. 2. Traditionally, it is recommended to use two receivers (see Fig. 2a) to improve the measurement accuracy of the LCR stress measurement system [8]. This tandem-catch arrangement minimises ToF measurement errors created by transmitter triggering uncertainty, wave speed changes in the transducers/wedge and material texture effects. The single element transducers (Fig. 2a) are replaced by two 10 MHz arrays with 16 elements (Fig. 2b). The transmitter array can generate 16 ultrasonic waves (T1-T16) and each of them can be received by any of the 16 elements of the receiver array (R1 -R16). Therefore, a matrix of  $16 \times 16$  LCR Paths can potentially be generated. Each of these 256 LCR paths is different from the

others (i.e., different distance or different position of the travel path in the material) whereby 256 ToFs can be generated. This is anticipated to increase the measurement accuracy in comparison with the traditional setup in which only two LCR Paths (LCR Path 1&2 in Fig. 2a) can be generated by the single element transducers.

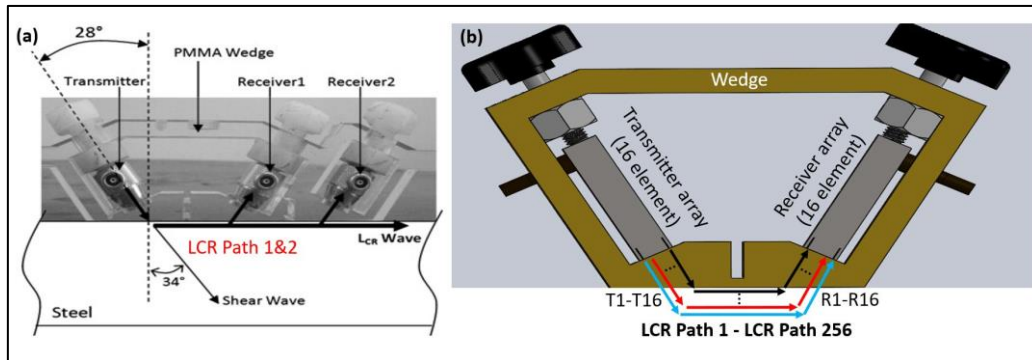


Fig. 2. (a) Traditional ultrasonic LCR stress measurement [8] and (b) PAUT-LCR stress measurement approach developed in this paper

### 3. Experimental setup and system requirements

#### 3.1. PAUT probes

An important challenge of the ultrasonic stress measurement method is the problem of average data measurement, i.e., an average of the residual stress in the area affected by the wave travel path is measured rather than point-based measurement [8, 12]. For example, the residual stress measured by 2 MHz transducers in 3 mm depth, see Fig. 1b, can include both surface and bulk stress data. Because the residual stress can change rapidly, especially in welded and WAAM components, the averaging issue is considered a major disadvantage of the ultrasonic residual stress measurement in the weld and WAAM [12]. There are some techniques to deal with this problem such as the FELCR method (combination of finite element welding simulation and LCR stress measurement) introduced by Javadi et al [8], increasing the number of measurement frequencies [13] in the application of both contact and immersion ultrasonic methods [14]. The size of the probe is also critical for the measurement of welding and WAAM residual stress whose sharp gradient will be impossible to be evaluated, in the case of using larger arrays, due to the averaging issue. Imasonic (France) small-footprint arrays are the smallest commercially available arrays and are used in this paper. They cover an area of 6x6.5 mm (see Fig. 3a) and have an active length ( $L$  in Fig. 3b) of only 3.9 mm. Two different frequencies of 5 MHz and 10 MHz are used in this work. Respectively, the 5 MHz and 10 MHz arrays have 8 elements with pitch 0.5mm and 16 elements with pitch 0.25 mm (dimension  $p$  in Fig. 3b).

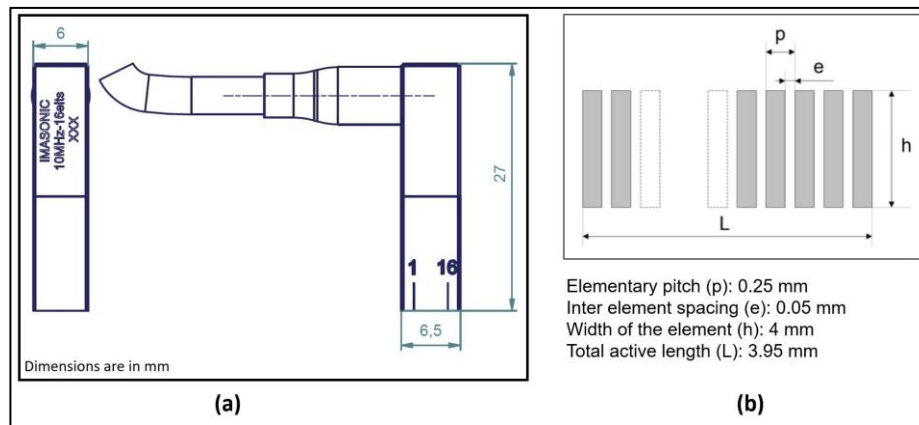


Fig. 3. (a) Mechanical drawing and (b) elements layout of the Imasonic Small-footprint array [image produced by Imasonic]

### 3.2. PAUT-LCR wedge design

The LCR waves are longitudinal bulk waves that travel parallel to the surface. Based on Snell's law, if the incident angle in the interface between two materials is equal to the first critical angle, the angle of refraction would be 90° and the wave will be propagated parallel to the surface. For example, the LCR wedge made of PMMA (with sound speed of 2757 m/s), which was used to measure the RS in stainless steel (with sound speed of 5800 m/s), had an angle of 28° (see Fig. 2a).

In this paper, the wedges are manufactured using waterjet cutting and machining processes. There is a slot designed in the centre of the wedge (see Fig. 4a) to ensure the wave produced by the transmitter array will be propagated in the specimen, and not in the wedge, before being received by the receiver array. Because couplant is used between the array and the wedge, it is necessary to apply constant mechanical force to the array to maintain surface contact. This is implemented using plastic screws as shown in Fig. 4b.

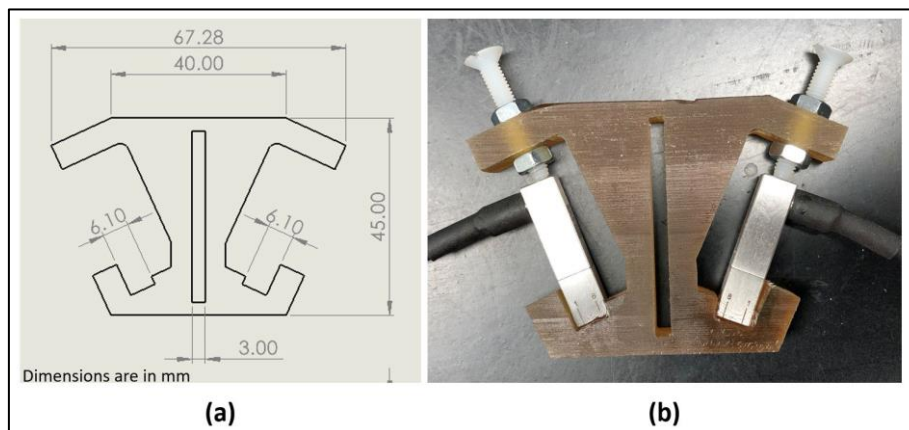


Fig. 4. (a) Mechanical drawing of the PAUT-LCR wedge and (b) the manufactured wedge and using the plastic screws to install the arrays

### 3.3. Robotic inspection

One of the main advantages of the PAUT system compared to the single element transducers, is the possibility of robotic inspection. Although the automation of the single element transducers is also possible, the PAUT system has been extensively used in the recent development of robotic NDE. For example, the system developed by the Center for Ultrasonic Engineering (CUE) at the University of Strathclyde for in-process inspection of welding and

WAAM relies on a robotic PAUT system, as described by Javadi et al [1, 15-17], Mohseni et al [18] and Vithanage et al [19]. Therefore, the requirements of robotic residual stress measurement using a PAUT system are also investigated in this paper.

The robotic PAUT-LCR system, shown in Fig. 5a, includes a 6-axis KUKA robot, phased array controller (LTPA by PEAK NDT, UK) and PAUT-LCR end-effector. The end-effector is mounted on the robot using a 3D printed holder and includes two 5 MHz arrays installed in the wedge. The specimen is a steel plate manufactured by robotic welding (multi-pass TIG welding) and its residual stress have been measured by the hole-drilling method as described by Javadi et al [1]. It is then known that the specimen contains a stress-free zone in the parent material (Fig. 5b), compressive stress in Heat Affected Zone (HAZ) (Fig. 5c) and high tensile stress in the weld (Fig. 5d). The PAUT-LCR end-effector is then moved by the 6-axis robot to measure the ToF in the parent material, HAZ and weld.

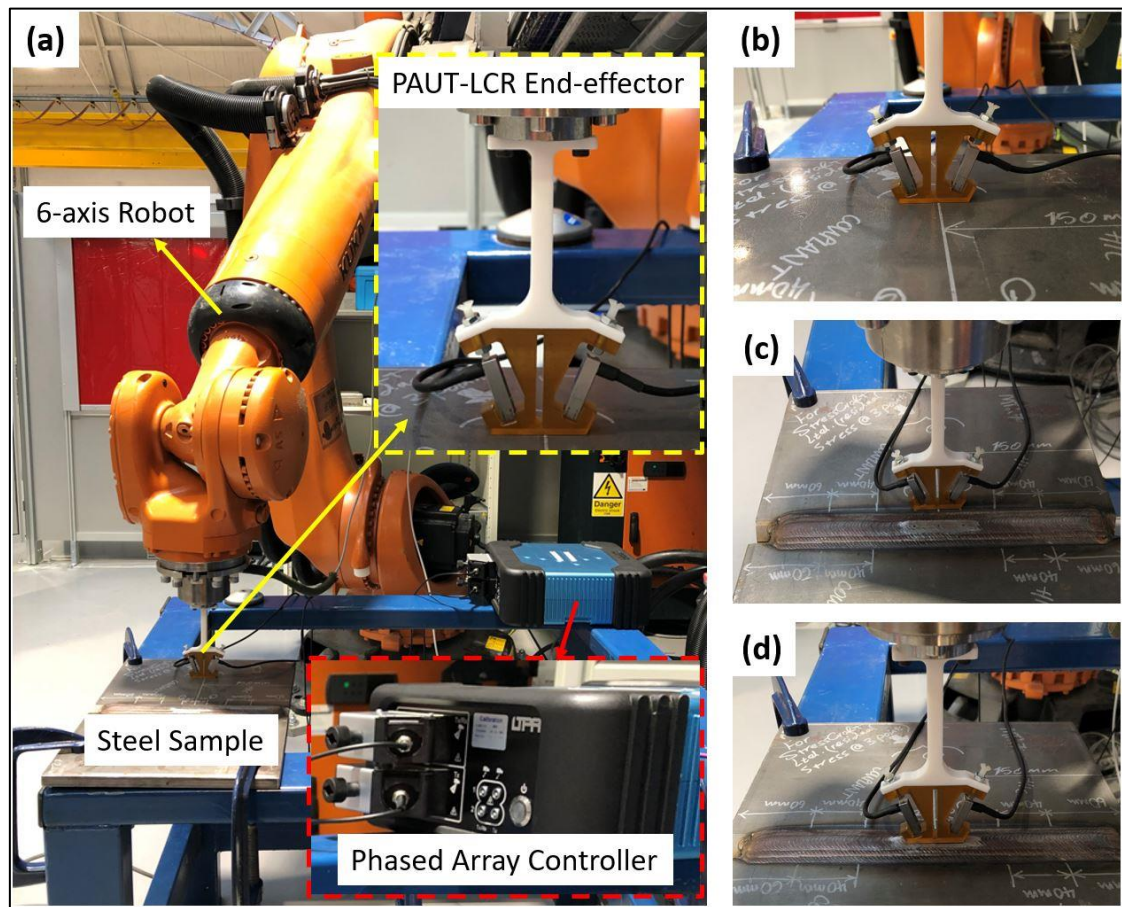


Fig. 5. (a) Robotic PAUT-LCR system and ToF measurement on (b) Parent Material, (c) HAZ and (d) Weld

Although the LCR waves are the most sensitive ultrasonic waves to residual stress, other types of ultrasonic waves were also investigated in residual stress applications by Egle and Bray [11] and the second most sensitive wave was the longitudinal (normal) wave. Therefore, the normal waves are also considered in this paper but with using the PAUT probes instead of the single-element transducers. The experimental setup, shown in Fig. 6, includes the phased array controller and two arrays which are installed on either side of the component, facing each other, using a 3D printed holder. The specimen was a WAAM component made of aluminium as described by Javadi et al [20].



Fig. 6. PAUT system for the residual stress measurement in the WAAM sample

#### 4. Results and Discussions

The LCR wave is the first signal received by the receiver transducer, unlike other wave modes such as the transversal wave, as it travels parallel to the surface through the shortest direct distance between the transmitter and receiver. This is usually the main method used to differentiate the LCR wave from other ultrasonic waves [8]. Therefore, the ToF from the transmitter to the receiver can be calculated based on the travel distance in the wedge and specimen if the sound velocity is known in both mediums. In the PAUT-LCR wedge, the travel distance needs to be calculated for each of the combinations of the transmitter and receiver elements. For example, calculating the travel distance in the wedge for  $T_1R_1$ ; the LCR wave sent by the first element of the transmitter and received by the first element of the receiver is equal to  $2 \times 5.4$  mm in the wedge and 24.42 mm in the specimen (see Fig. 7). The sound velocity was measured to be 2470 m/s and 5890 m/s in the wedge and steel sample, respectively. Therefore, the ToF for  $T_1R_1$  is calculated to be 8.4  $\mu$ s. Accordingly, the ToF for  $T_4R_4$  and  $T_8R_8$  (Fig. 7) was also calculated to be 8.4  $\mu$ s. Therefore, the ToF for the PAUT-LCR wave is consistent regardless of the LCR path and combination of element number of the transmitter and receiver. This claim can be geometrically proved based on Snell's law and assumptions shown in Fig. 8. The ToF of the wave generated by  $T_8$  (element number 8) which travels in the wedge by a distance of  $A_2$ , is equal to  $A_2/V_1$  where  $V_1$  is the velocity of sound in the wedge. Similarly, this is equal to  $A_1/V_1$  for  $T_1$  (element number 1). The ToF of the LCR wave travelling in the steel sample from the incident point of  $T_1$  to the incident point of  $T_8$  (distance of  $T + B_2$ ) is equal to  $(T + B_2)/V_2$  where  $V_2$  is the velocity of sound in the steel sample. If  $A_2/V_1$  is equal to  $A_1/V_1 + (T + B_2)/V_2$ , then the ToF is consistent along all paths, regardless of the number of elements in the transmitter array (shown in Fig. 8). The same proof can be used to show the independence of ToF and element number in the receiver. The ToF from the incident point of  $T_8$  to the incident point of  $R_8$  is also the same for all other combinations of the transmitter and receiver elements. Therefore, it can be concluded that the ToF of the PAUT-LCR is always consistent. This was experimentally observed in this work as the phased array controller allowed monitoring of various combinations, two of 64 waves generated are shown in Fig. 9, which all had the same ToF results.

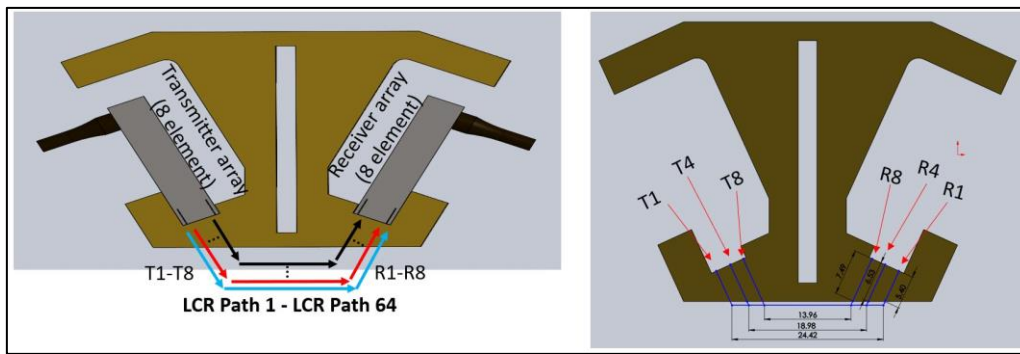


Fig. 7. LCR Path distance in the PAUT-LCR system

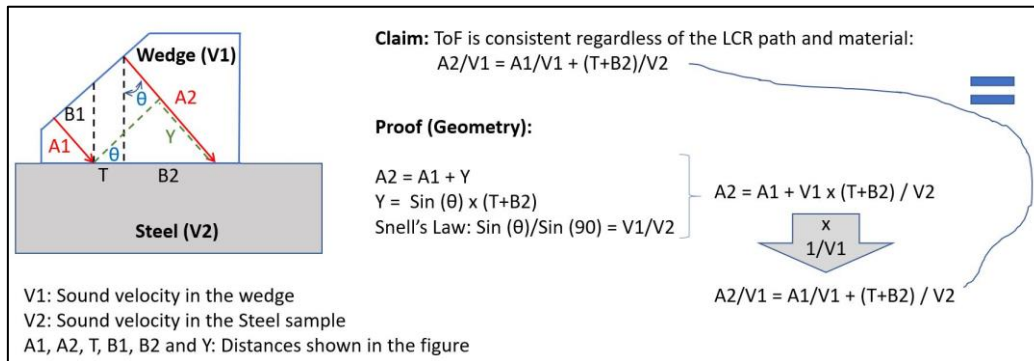


Fig. 8. Geometrical proof for the ToF consistency regardless of the number of element

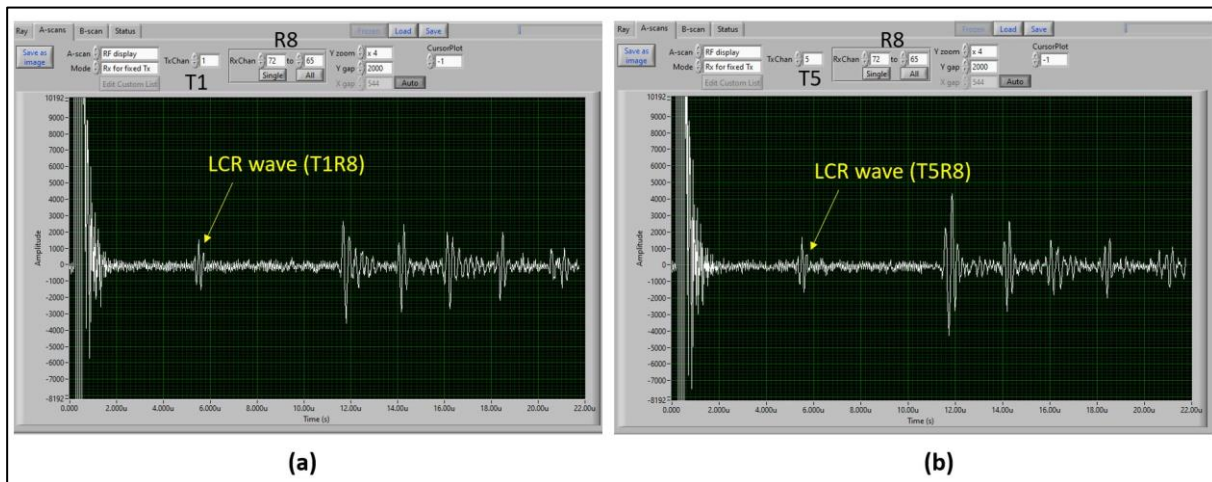


Fig. 9. PAUT-LCR waves generated by two combinations of the element numbers: (a) T1R8 and (b) T5R8

The PAUT-LCR system also detected ToF variations in the parent material, HAZ and weld showing the potential of this method for residual stress measurement. However, it can be seen in Fig. 9 that the LCR wave amplitude is weak and was even weaker in the weld. This was expected as the same weak signals had been reported in weld inspection using the single-element transducers method [8]. Therefore, it is important to have an alternative inspection methodology such as the normal waves used in this work (shown in Fig. 10). ToF variations were also detected using this PAUT normal wave approach in different positions of the WAAM sample. Since the travel distance (WAAM component thickness) is consistent, the ToF variation is representing the material texture and the residual stress. However, it should be noted that this is an initial development of the system while in a fully-developed system, it is necessary to

differentiate between material texture effects and residual stress using the stress-relieving process and acoustoelastic coefficient measurement.

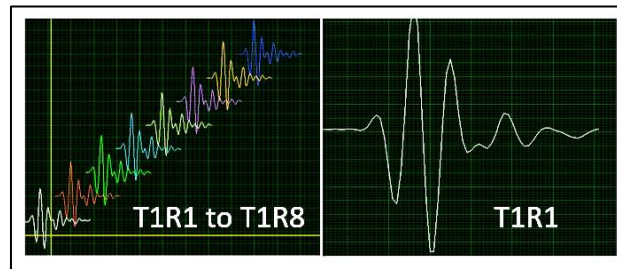


Fig. 10. PAUT normal wave results

## 5. Conclusions

In this paper, the feasibility of using a PAUT system for residual stress measurement was studied and based on the results, it can be concluded that:

- 1) The experimental setup and requirements of the PAUT-LCR system were successfully developed for ToF measurement in welded and WAAM components.
- 2) The ToF measured for the PAUT-LCR waves is consistent, regardless of the number of the triggering element in the transmitter array and/or receiving element in the receiver array.
- 3) The PAUT system can detect the ToF variations in the parent material, HAZ and weld as well as different areas of the WAAM component. This shows the potential of the method for residual stress measurement.
- 4) The PAUT-LCR waves have shown weak signals, especially in the weld. Alternative ultrasonic waves, like the normal waves tested in this paper, are required in conjunction with LCR waves to expand the capabilities for residual stress measurement.
- 5) The robotic deployment was at the core of all experiments conducted in this paper. This shows the potential of the PAUT system for the development of a robotic residual stress measurement system.

## References

- [1] Y. Javadi, N.E. Sweeney, E. Mohseni, C.N. MacLeod, D. Lines, M. Vasilev, Z. Qiu, C. Mineo, S.G. Pierce, A. Gachagan, Investigating the effect of residual stress on hydrogen cracking in multi-pass robotic welding through process compatible non-destructive testing, *Journal of Manufacturing Processes* (2020).
- [2] F. Martina, M.J. Roy, B.A. Szost, S. Terzi, P.A. Colegrove, S.W. Williams, P.J. Withers, J. Meyer, M. Hofmann, Residual stress of as-deposited and rolled wire plus arc additive manufacturing Ti-6Al-4V components, *Materials Science and Technology* 32 (2016) 1439-1448.
- [3] L. Pérez Caro, E.-L. Odenberger, M. Schill, F. Niklasson, P. Åkerfeldt, M. Oldenburg, Springback prediction and validation in hot forming of a double-curved component in alloy 718, *International Journal of Material Forming* (2021).
- [4] J.C. Outeiro, 11 - Residual stresses in machining, in: V.V. Silberschmidt (Ed.), *Mechanics of Materials in Modern Manufacturing Methods and Processing Techniques*, Elsevier2020, pp. 297-360.
- [5] P.J. Withers, Residual stress and its role in failure, *Reports on Progress in Physics* 70 (2007) 2211-2264.
- [6] J. Hönnige, C.E. Seow, S. Ganguly, X. Xu, S. Cabeza, H. Coules, S. Williams, Study of residual stress and microstructural evolution in as-deposited and inter-pass rolled wire plus arc

additively manufactured Inconel 718 alloy after ageing treatment, *Materials Science and Engineering: A* 801 (2021) 140368.

[7] J.A. Francis, H.K.D.H. Bhadeshia, P.J. Withers, Welding residual stresses in ferritic power plant steels, *Materials Science and Technology* 23 (2007) 1009-1020.

[8] Y. Javadi, M. Akhlaghi, M.A. Najafabadi, Using finite element and ultrasonic method to evaluate welding longitudinal residual stress through the thickness in austenitic stainless steel plates, *Materials & Design* 45 (2013) 628-642.

[9] ASTM, Standard Test Method for Determining Residual Stresses by the Hole-Drilling StrainGage Method, ASTM E837-13a, ASTM, West Conshohocken, PA, United States, 2013., pp. 1-16.

[10] M.B. Prime, M.R. Hill, A.T. DeWald, R.J. Sebring, V.R. Dave, M.J. Cola, Residual stress mapping in welds using the contour method, *Trends in Welding Research, Proceedings* (2003) 891-896.

[11] D.M. Egle, D.E. Bray, Measurement of acoustoelastic and third-order elastic constants for rail steel, *The Journal of the Acoustical Society of America* 60 (1976) 741-744.

[12] Y. Javadi, M. Ashoori, Sub-surface stress measurement of cross welds in a dissimilar welded pressure vessel, *Materials & Design* 85 (2015) 82-90.

[13] Y. Javadi, M. Akhlaghi, M.A. Najafabadi, Nondestructive Evaluation of Welding Residual Stresses in Austenitic Stainless Steel Plates, *Research in Nondestructive Evaluation* 25 (2014) 30-43.

[14] Y. Javadi, M.A. Najafabadi, M. Akhlaghi, Comparison between Contact and Immersion Method in Ultrasonic Stress Measurement of Welded Stainless Steel Plates, *Journal of Testing and Evaluation* 41 (2013) 788-797.

[15] Y. Javadi, E. Mohseni, C.N. MacLeod, D. Lines, M. Vasilev, C. Mineo, S.G. Pierce, A. Gachagan, High-temperature in-process inspection followed by 96-h robotic inspection of intentionally manufactured hydrogen crack in multi-pass robotic welding, *International Journal of Pressure Vessels and Piping* 189 (2021) 104288.

[16] Y. Javadi, E. Mohseni, C.N. MacLeod, D. Lines, M. Vasilev, C. Mineo, E. Foster, S.G. Pierce, A. Gachagan, Continuous monitoring of an intentionally-manufactured crack using an automated welding and in-process inspection system, *Materials & Design* 191 (2020) 108655.

[17] Y. Javadi, N.E. Sweeney, E. Mohseni, C.N. MacLeod, D. Lines, M. Vasilev, Z. Qiu, R.K.W. Vithanage, C. Mineo, T. Stratoudaki, S.G. Pierce, A. Gachagan, In-process calibration of a non-destructive testing system used for in-process inspection of multi-pass welding, *Materials & Design* 195 (2020) 108981.

[18] E. Mohseni, Y. Javadi, N.E. Sweeney, D. Lines, C.N. MacLeod, R.K.W. Vithanage, Z. Qiu, M. Vasilev, C. Mineo, P. Lukacs, E. Foster, S.G. Pierce, A. Gachagan, Model-assisted ultrasonic calibration using intentionally embedded defects for in-process weld inspection, *Materials & Design* 198 (2021) 109330.

[19] R.K.W. Vithanage, E. Mohseni, Z. Qiu, C. MacLeod, Y. Javadi, N. Sweeney, G. Pierce, A. Gachagan, A Phased Array Ultrasound Roller Probe for Automated in-Process/Interpass Inspection of Multipass Welds, *IEEE Transactions on Industrial Electronics* 68 (2021) 12781-12790.

[20] Y. Javadi, C.N. MacLeod, S.G. Pierce, A. Gachagan, W. Kerr, J. Ding, S. Williams, M. Vasilev, R. Su, C. Mineo, J. Dziejewicz, Ultrasonic phased array inspection of wire plus arc additive manufacture (WAAM) samples using conventional and total focusing method (TFM) imaging approaches, *Insight* 61 (2019) 144-148.